A Morphological Study of the Formation of PdH_x on Thin Palladium Films

Marcin Fiałkowski,*,† Robert Nowakowski,† and Robert Hołyst†,‡

Institute of Physical Chemistry, Polish Academy of Sciences, Kasprzaka 44/52, 01-224 Warsaw, Poland, and Department of Mathematics and Natural Sciences, College of Science, Cardinal Stefan Wyszyński University, Dewajtis 5, 01-815 Warsaw, Poland

Received: March 7, 2003; In Final Form: March 17, 2004

We propose a mechanism for the creation of the two-dimensional ridge pattern morphology during the formation of palladium hydride on the surface of thin palladium films at 298 K. Expressions for the distribution of domain areas and circumferences, derived from the maximum entropy principle, are in very good agreement with experiment.

1. Introduction

Cellular structures in 2D are known in many areas of science.[1] Whether we consider bee's honeycomb, soap foam (or froth),[2−4] defects condensation of charge density waves,[5] territory of fire ants,[6] administrative divisions,[7,8] superclusters of galaxies (large scale structure of the universe),[9] 2D sections of polycrystalline materials, chemical patterns on surfaces, and crack structure in ceramics,[10] we find characteristic morphological patterns. Such pattern subjected to the detailed quantitative morphological analysis, as in the case of 2D transition in magnetic systems,[11] or kinetic roughening of the etched Si[12] can give information about the mechanisms of their formation and characteristics of the distribution of the domains. This in turn may be useful in the characterization of the given material by its two-dimensional surface pattern.

Cellular structures are also observed on thin metal films during the process of formation of metal hydrates. It has recently been shown[13] that the absorption of hydrogen on Gd films is accompanied by the formation of a characteristic surface pattern caused by dislocation loops and misfit dislocations at the interface between the substrate and the film. Similar morphological changes, occurring on thin Pd films deposited on glass substrate in hydrogen atmosphere have also been reported by Nowakowski et al.[14,15] The creation of the ridge pattern on the palladium surface is driven by the formation of palladium hydride (PdH_x) sites on defects present in the surface−substrate region. Recently, the AFM/video techniques were used[15] to compare the ridge patterns formed on Pd films deposited on two kinds of substrates: on glass with randomly distributed defects, and on a well-ordered mica substrate with steps and terraces defects. These experiments revealed differences in the pattern morphology indicating the role of substrate in the process of the generation of active sites in PdH_x formation/relaxation process. However, the mechanism of the creation of the ridge pattern during the formation is far from being understood.

We present here experimental and theoretical studies of the absorption of hydrogen in the thin Pd films deposited on atomically flat mica substrate. It is our goal to propose a mechanism for the creation of the two-dimensional ridge pattern during the formation of palladium hydride on the surface of palladium film. We will seek to characterize the morphology of this pattern in terms of the distributions of the domain areas and circumferences. We apply the maximum entropy principle and assume that the entropy of the domain pattern is maximized, subject to certain geometrical constraints. We shall demonstrate that the form of the constraints can be inferred from the mechanism governing the pattern formation.

The rest of the paper is organized as follows: In the next section the experimental part of our work is described. In section 3 the maximum entropy principle (MEP) is formulated for the system under consideration. The formulas for the distributions of domain areas and circumferences are derived. In section 4 the predictions drawn from the MEP are compared with experimental data. Summary of the results and final remarks are given in the concluding section 5.

2. Experimental Section

In the course of the experimental work thin Pd films were deposited under UHV conditions (10^{-8} Pa) on the freshly cleaved mica, maintained at 78 K by evaporation of fine Pd wires from a tungsten heater. After the film deposition, the samples were sintered at 370 K for 20 min under UHV conditions, and then cooled to the room temperature. Finally, the samples were taken out of the UHV apparatus and put into the AFM reactor. The AFM was first used for the determination of the film thickness after appropriate scratching (average film thickness was 40 nm). The formation of PdH_x was induced by the H_2 flow over the Pd film at the temperature 298 K under the pressure 101 kPa. The equilibrium pressure of hydrogen at 298 K over $PdH_{0.5}$ is 1 kPa. As a result, a system of ridges was created on the surface of the palladium film. The reactor connected with the gas dosing system enabled in situ video/AFM investigations[15] of the phenomena occurring on the surface during the flow of gases. The average height of the ridges was about 1.5 μm. The creation of ridges forming a network structure was a stable plastic deformation, which enabled us to observe it over a large area by means of an optical microscope. The image of the pattern formed on the film surface used in our further morphological analysis, shown in Figure 1.

3. Theory

In this section we propose a mechanism to explain metric properties of the ridge pattern created on the palladium plate

† Polish Academy of Sciences.
‡ Cardinal Stefan Wyszyński University.

10.1021/jp034593m CCC: $27.50
Published on Web 04/28/2004

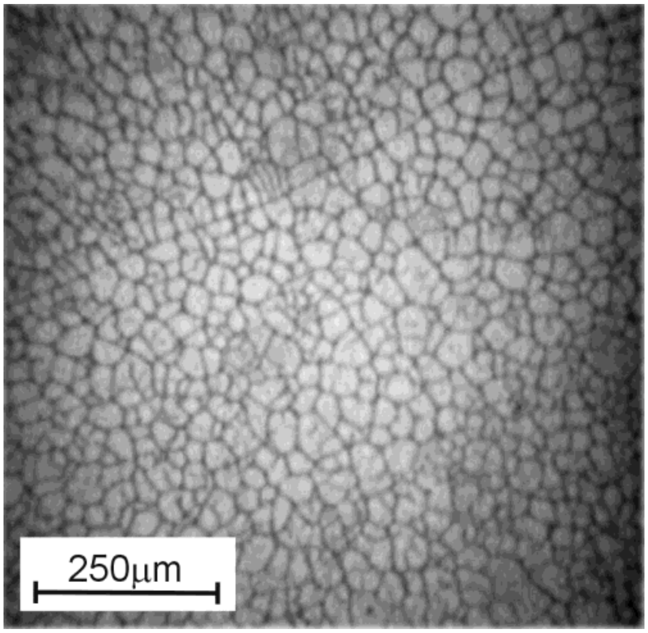

Figure 1. Network of ridges resulting from the PdH_x formation on palladium thin film observed under an optical microscope. The average height of the ridges is about 1.5 μm.

during the formation of PdH_x. Our approach is based on the maximum entropy conjuncture. We will argue that the observed system of ridges takes up the most random form subject to the constraints resulting from the nature of physical processes underlying the pattern formation.

The absorption of hydrogen is related to the increase of the size of the elementary cell of the palladium lattice. As a result, the volume of the film increases by a certain factor λ. The excess volume gives rise to internal stresses that relax by releasing some amount of volume on the surface of the plate in the form of the ridge. In this way the surface of the metal is successively covered with a system of random ridge lines. The process stops when the molar fraction of hydrogen reaches its equilibrium value. Denote the amount of volume associated with the unit length of the ridge by β. Then the balance equation relating the total area of the surface exposed to hydrogen, A_{tot}, and the total length of the ridge lines, L_{tot}, is written as

$$\lambda A_{\mathrm{tot}} = \beta L_{\mathrm{tot}} \tag{1}$$

The domain pattern formed on the surface of palladium is determined by the system of ridges and is characterized by the probability $f(L)$ of finding a domain of the circumference equal to L. Following the conjecture made by Jaynes,[16] we assume that the most probable distribution of the circumferences maximizes the entropy given by the functional

$$S = -\int f(l) \ln f(l)\, \mathrm{d}l \tag{2}$$

subject to the constraint imposed by the balance equation, eq 1. In the above equation the distribution function $f(l)$ refers to the reduced circumference, $l = L/\langle L\rangle$, where $\langle L\rangle$ is the average domain circumference in the system.

The second variable used to characterize the metric properties of a domain is the reduced area, a, defined as $a = A/\langle A\rangle$, where A is the area of the domain and $\langle A\rangle$ is the mean area in the system. In terms of the distributions $f(l)$ and $f(a)$ the constraint (1) can be written as $\lambda\langle A\rangle\int f(a)a\, \mathrm{d}a = {}^1/_2\beta\langle L\rangle\int f(l)l\, \mathrm{d}l$. The factor $^1/_2$ is due to the fact that the borderline belongs to two domains. We have also $\langle L\rangle = L_{\mathrm{tot}}/2N$ and $\langle A\rangle = A_{\mathrm{tot}}/N$, with N being the number of domains in the system. If we make use of the fact that the variables a and l are not independent, but are linked by the power relation

$$a = \eta l^{\nu} \tag{3}$$

where $\nu = 2$ and η is some constant, the constraint (1) takes the following form:

$$\int f(l)(l^2 - \gamma l)\, \mathrm{d}l = 0 \tag{4}$$

where $\gamma = \beta\langle L\rangle/2\lambda\eta\langle A\rangle$. Two additional constraints imposed on the distribution $f(l)$ follow from the normalization conditions,

$$\int f(l)\, \mathrm{d}l = N \tag{5}$$

$$\int f(l)l\, \mathrm{d}l = 1 \tag{6}$$

The maximization procedure of the entropy functional (2) with the constraints (4), (5), and (6) yields the distribution of the domain circumferences in the form of the Gaussian distribution,

$$f(l) = \frac{N}{\sqrt{2\pi\sigma_l^{\,2}}} \exp\left[-\frac{(l-\mu_l)^2}{2\sigma_l^{\,2}}\right] \tag{7}$$

with $\mu_l = 1$ and $\sigma_l = \sqrt{\gamma - 1}$. The variable l takes only positive values. Therefore, the formula (7) is valid when the standard deviation σ_l is sufficiently small, i.e., $\sigma_l \lesssim {}^1/_3$.

The distribution of domain areas, $f(a)$, can be obtained from $f(l)$ by changing the variables according to relation (3), i.e., $f(a) = f(l(a))\, \mathrm{d}l(a)/\mathrm{d}a$. It has the following form:

$$f(a) = \frac{N}{n(\mu_a,\sigma_a)}\sqrt{a}\, \exp\left[-\frac{(\sqrt{a}-\mu_a)^2}{2\sigma_a^{\,2}}\right] \tag{8}$$

where the normalizing factor, $n(\mu_a,\sigma_a)$, is given by the formula

$$n(\mu_a,\sigma_a) = \sqrt{2\pi\sigma_a^{\,2}}(\sigma_a^{\,2} + \mu_a^{\,2})\left[1 + \mathrm{erf}\left(\frac{\sqrt{2}\mu_a}{2\sigma_a}\right)\right] + 2\sigma_a^{\,2}\mu_a \exp\left(-\frac{\mu_a^{\,2}}{2\sigma_a^{\,2}}\right) \tag{9}$$

In the next section we compare the predictions about the distributions of domain circumferences and areas, eqs 7 and 8, with experimental data.

4. Comparison with Experiment

In our study we analyzed the digital image of palladium plate covered with a ridge pattern (Figure 1) taken using an optical microscope. The domain boundaries are determined by the network of the ridge lines. In the first step, to obtain a skeleton of the domain structure, the boundaries of the domains were approximated by straight lines. As a result, a mosaic composed of irregular polygons shown in Figure 2 was obtained. The metric properties of this structure (areas and circumferences of individual polygons) were characterized with the help of our software[17,18] developed for two-dimensional morphological analysis. The total number of domains taken into account in the statistical analysis presented in this section was $N = 655$.

Frequency distribution of the reduced domain circumferences $l = L/\langle L\rangle$ are shown in Figure 3. The average domain circumference is $\langle L\rangle = 109.1$ μm. The data were grouped into

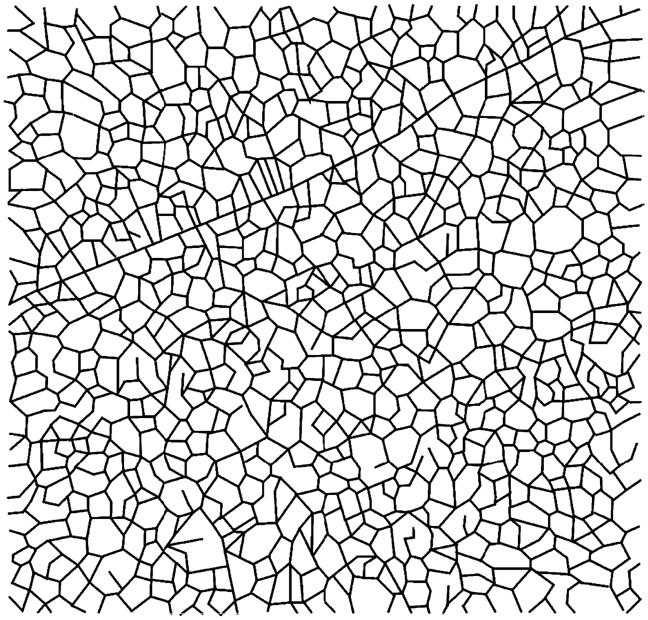

Figure 2. System of polygons obtained from the original image of the ridge pattern shown in Figure 1. The domain boundaries have been approximated by straight lines.

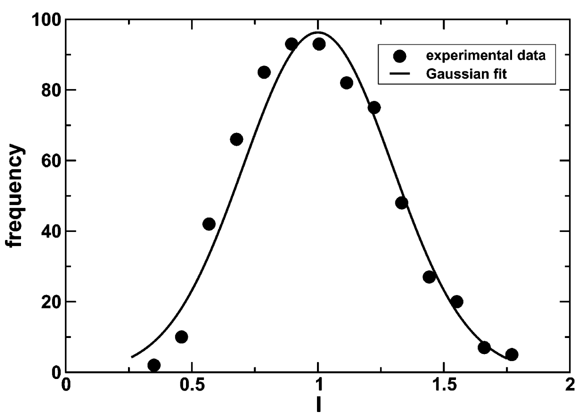

Figure 3. Frequency distribution $f(l)$ of the reduced domain circumferences, $l = L/\langle L\rangle$. The continuous line represents the least-squares fit corresponding to the Gaussian distribution, eq 7, to experimental data.

12 intervals of equal size $\Delta l = 0.1092$ and two outer intervals: $l < 0.4044$ and $l > 1.7148$. The least-squares fit of the Gaussian distribution (eq 7) to experimental data yields the parameter (standard deviation) $\sigma_l = 0.296 \pm 0.011$. Note here also that the interval from $l = 0$ to $l = 1$ (mean) is wider than $3\sigma_l$. Therefore, the domain of the distribution given by eq 7 can be perfectly approximated by the interval $(-\infty, +\infty)$.

To check whether the frequencies shown in Figure 3 follow the Gaussian distribution, the χ^2 goodness-of-fit test[19] has been carried out. The χ^2 statistic is defined as

$$\chi^2 = \sum_i^k \frac{(n_i - e_i)^2}{e_i} \tag{10}$$

where k is the number of bins, n_i and e_i are respectively the observed and expected frequencies for the ith bin. The expected frequency is calculated by $e_i = N(F(x_u) - F(x_l))$, where F is the cumulative distribution function for the distribution being tested, x_u is the upper limit for bin i, x_l is the lower limit for bin i, and N is the sample size. The null hypothesis that the testing distribution fits the data is accepted if the value of χ^2 is less than critical value corresponding to a chosen significance level.

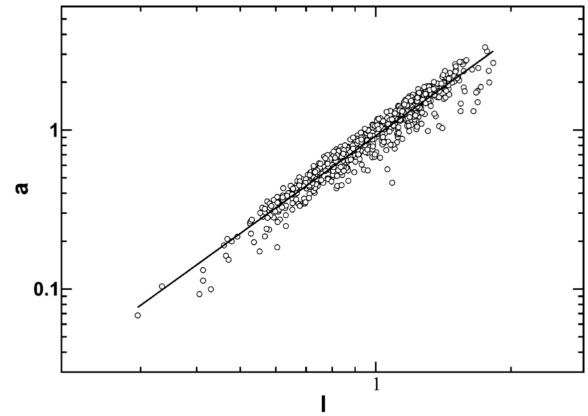

Figure 4. Dependence of the reduced domain circumferences, $l = L/\langle L\rangle$, on the reduced domain areas, $a = A/\langle A\rangle$, plotted on the log−log scale. The average domain circumference and the average domain area are respectively $\langle L\rangle = 109.1$ μm and $\langle A\rangle = 698.3$ μm.[2] Data for $N = 655$ domains are shown. The least-squares fit to the function $a = \eta l^{\nu}$ (plotted with a solid line) yields $\eta = 0.9189 \pm 0.0057$ and $\nu = 2.039 \pm 0.021$.

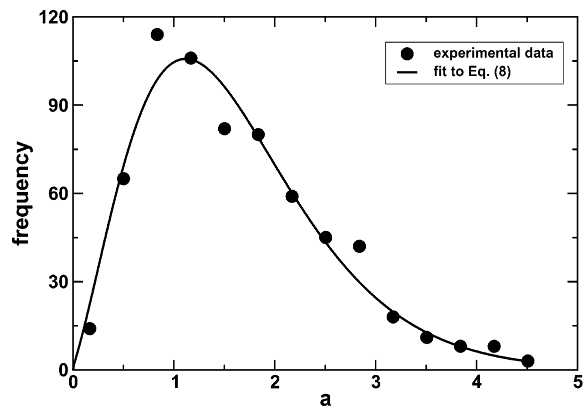

Figure 5. Frequency distribution $f(a)$ of the reduced domain areas, $a = A/\langle A\rangle$. The continuous line represents the least-squares fit of the distribution function given by eq 8 to experimental data.

For the Gaussian distribution given by eq 7 fitted to the histogram of circumferences the χ^2 test statistic is $\chi^2 = 23.81$. The critical value of the χ^2 distribution with 12 degrees of freedom for the significance level $\alpha = 0.02$ is $\chi^2_{(0.02,12)} = 24.05$. It follows that the null hypothesis that the Gaussian function approximates the observed frequency distribution is accepted.

In Figure 4 the reduced domain areas, a, are plotted against the reduced domain circumferences, l. The fit of the power relation (3) to the data points yields $\eta = 0.9189 \pm 0.0057$ and $\nu = 2.039 \pm 0.021$. This result justifies the form of the distribution $f(a)$ that is derived from the distribution of domain circumferences, $f(l)$, on the basis of the exponent $\nu = 2$.

Frequency distribution of the reduced domain areas $a = A/\langle A\rangle$ is shown in Figure 5. The calculated average domain area is $\langle A\rangle = 698.3$ μm^2. The data are divided into 13 bins of equal size $\Delta a = 0.3339$ (covering the interval from 0 to 4.3410) and one outer bin for $a > 4.3410$. The least-squares fit of the distribution given by eq 8 to the observed frequency distribution gives $\mu_a = 0.893 \pm 0.034$ and $\sigma_a = 0.416 \pm 0.021$. To determine whether the distribution given by eq 8 provides a good fit to observed data, the χ^2 test has also been used. The calculated value of the χ^2 statistic is $\chi^2 = 17.73$. The critical value of the χ^2 distribution with 11 degrees of freedom for the significance level $\alpha = 0.05$ is $\chi^2_{(0.05,11)} = 19.68$. It means that the hypothesis that the distribution of domain areas is described by eq 8 is accepted.

5. Summary and Conclusions

In this paper we have investigated the morphology of the ridge pattern formed in the palladium thin film absorbing hydrogen. We have proposed a mechanism to explain the observed metric properties of the domain pattern, which is determined by the network of ridges. Our approach is based on the maximum entropy principle. We have assumed that the observed domain pattern takes up the most disordered form subject to specific constrains following from the nature of the physical processes governing the pattern formation. The constraints account for the fact that the amount of volume released on the surface in the form of the ridges is proportional to the excess volume caused by the absorption of hydrogen. From the maximum entropy principle we have derived formulas for the distribution of domain areas and circumferences. The χ^2 goodness-of-fit tests showed that the theoretical distributions agree very well with the experimental data at a statistically significant level: $\alpha = 0.02$ for the distribution of domain circumferences and $\alpha = 0.05$ for the distribution of domain areas.

The absorption and migration of gases in metals plays an important role in many fields of science and technology. One of the issues studied experimentally is the number of gases that can be stored inside the solid.[20] The absorption of hydrogen is of primarily importance as it is believed that solids offer a possibility of the safe storage of hydrogen used as a fuel. The effect of the hydrogen absorption in solids results in deformation processes. Such deformation may have a desirable effect on solid properties such as in the case of the controlled hole opening in the membrane arrays of Pd obtained in the two-step replication of anodic porous aluminia.[21] Moreover the amount of the absorbed hydrogen inside a solid depends on the existing deformations inside a solid: it has been shown that in metallic glasses and amorphous materials the capacity for the absorption of hydrogen is greater than in the crystalline counterpart.[22,23] The absorption of hydrogen influences also the corrosion fatigue[24] and interfacial structures of materials.[25] The plastic deformations of the material subjected to the influence of hydrogen can give us a hint about a possible mechanism of the absorption and diffusion inside a solid. It also can tell us about the distribution of hydrogen in the material.

One may expect that the morphology class characterized by the distribution $f(l)$ given by eq 7 is generic for two-dimensional patterns observed on different kinds of metal plates absorbing gases. In particular, it remains an open question whether the calculated value of the parameter $\sigma_l \approx 0.3$, describing the characteristic size distribution of the domains, is typical for a wider class of absorption processes occurring on the metal surface.

Acknowledgment. This work has been supported by the KBN under Grant 2P03B00923. The authors thank Prof. R. Duś for useful discussions and for a critical reading of the manuscript. M.F. acknowledges financial support from the NATO Scientific Fellowship.

References and Notes

(1) Weaire, D.; Rivier, N. *Contemp. Phys.* **1984**, *25*, 59.
(2) Stavans, J.; Glazier, J. A. *Phys. Rev. Lett.* **1989**, *62*, 1318.
(3) Hamsy, A.; Paredes, R.; Sonneville-Aubrun, O.; Cabane, B.; Botet, R. *Phys. Rev. Lett.* **1999**, *82*, 3368.
(4) Kader, A. A.; Earnshaw, J. C. *Phys. Rev. Lett.* **1999**, *82*, 2610.
(5) Weitering, H. H.; Carpinelli, J. M.; Melechko, A. P.; Zhang, J. D.; Bartkowiak, M.; Plummer, E. W. *Science* **1999**, *285*, 2107.
(6) Adams, E. S. *Ecology* **1998**, *79*, 1125.
(7) Caër, G. L.; Delannay, R. *J. Phys. I Fr.* **1993**, *3*, 1777.
(8) Glass, L.; Tobler, W. R. *Nature* **1971**, *233*, 67.
(9) Coles, P. *Nature* **1990**, *346*, 446.
(10) Korneta, W.; Mendiratta, S. K.; Menteiro J. *Phys. Rev. E* **1998**, *57*, 3142.
(11) Fiałkowski, M.; Hołyst, R. *Phys. Rev. E* **2002**, *66*, 046121.
(12) Dotto, M. E. R.; Kleinke, M. U. *Physica A* **2001**, *295*, 149.
(13) Pundt, A.; Getzlaff, M.; Bode, M.; Kirchheim, R.; Wiesendanger, R. *Phys. Rev. B* **2000**, *61*, 9964.
(14) Nowakowski, R.; Grzeszczak, P.; Duś, R. *Surf. Sci.* **2002**, *507*, 813.
(15) Nowakowski, R.; Duś, R. *Langmuir* **2003**, *19*, 6750.
(16) Jaynes, E. T. *Phys. Rev.* **1957**, *106*, 620; Jaynes, E. T. *Phys. Rev.* **1957**, *108*, 171.
(17) Aksimentiev, A.; Fiałkowski, M.; Hołyst, R. *Adv. Chem. Phys.* **2002**, *121*, 141.
(18) Free software for 2D and 3D morphological analysis is available on www.ichf.edu.pl/morph.html.
(19) Eadie, W. T.; Dryard, D.; James, F. E.; Roos, M.; Sadoulet, B. *Statistical Methods in Experimental Physics*; North-Holland, Amsterdam 1971.
(20) Mori, W.; Inoue, F.; Yoshida, K.; Nakayama, H.; Takamizawa, S.; Kishita, M. *Chem. Lett.* **1997**, *12*, 1219.
(21) Masuda, H.; Fukuda, K. *J. Electroanal. Chem.* **1999**, *473*, 240.
(22) Zhang, L. T.; Ito, K.; Vasudevan, V. K.; Yamaguchi, M. *Acta Mater.* **2001**, *49*, 751.
(23) Daewoong, S.; Asoka-Kumar, P.; Dauskardt, R. H. *Acta Mater.* **2002**, *50*, 537.
(24) Wang, Z. F.; Briant, C. L.; Kumar, K. S.; Wei, X. J.; Li, J.; Ke, W. *Mater. Trans. JIM* **1998**, *39*, 365.
(25) Li, X.; Wang, H.; Wang, W. N.; Tang, Y. J.; Zhao, H. W.; Zhan, W. S.; Hou, J. G. *J. Phys. Condens. Matter* **2001**, *13*, 3987.